


Article

Viability of an Open-Loop Heat Pump Drying System in South African Climatic Conditions [†]

Solomzi Marco Ngalonkulu *  and Zhongjie Huan

Department of Mechanical and Mechatronics Engineering, Tshwane University of Technology, Staatsartillerie Road, Pretoria West, Pretoria 0183, South Africa; huanz@tut.ac.za

* Correspondence: ngalonkulus@tut.ac.za

[†] This paper is an extended version of our paper published in 2023 International Heat Transfer Conference 17, Cape Town, South Africa, 14–18 August 2023; pp. 2948–2957.

Abstract: Drying agricultural produce consumes a considerable amount of energy. As an energy-efficient system, a heat pump can improve the energy efficiency of the drying process and hence reduce the energy consumption, especially in South Africa, where both sub-tropical and temperate weather conditions dominate. The objective of this research is to experimentally investigate the impacts of weather conditions on the operational conditions and thermal performance of an open-loop air-source heat pump drying system. The experimental investigation was conducted in a climate chamber where the climate conditions were simulated from -10°C to 20°C with an interval of 10°C for the typical temperature range of the harvesting season in South Africa. The findings indicate that ambient temperatures have a significant impact on both the operating conditions and thermal performance of an open-loop heat pump system; the change in ambient temperatures from -10°C to 20°C leads to a 141.6% improvement in the suction pressure, a 214.2% increase in the discharge pressure, and 30.1% increase in the compression ratio, as well as a consequent increase of 130.6% in the refrigerant mass flow rate (from 0.0067 to 0.0155 kg/s), resulting in a corresponding increase in the coefficient of performance (COP) of the heat pump drying system by about 42.1%. Therefore, this study suggests that, while using an open-loop air-source heat pump drying system utilising R134a refrigerant is feasible in South Africa, it may be practically limited to regions with warm climates or during warmer seasons.



Citation: Ngalonkulu, S.M.; Huan, Z. Viability of an Open-Loop Heat Pump Drying System in South African Climatic Conditions. *Energies* **2024**, *17*, 2432. <https://doi.org/10.3390/en17102432>

Academic Editor: Antonio Rosato

Received: 25 April 2024

Revised: 14 May 2024

Accepted: 17 May 2024

Published: 20 May 2024



Copyright: © 2024 by the authors. Licensee MDPI, Basel, Switzerland. This article is an open access article distributed under the terms and conditions of the Creative Commons Attribution (CC BY) license (<https://creativecommons.org/licenses/by/4.0/>).

Keywords: heat pump drying; ambient temperatures; thermal performance; mass flow rate; COP

1. Introduction

South Africa generates about 85% of its electricity from coal combustion, making it responsible for 42% of emissions in Africa, which is the largest emitter in Africa, the world's 11th most significant greenhouse gas emitter, and the most carbon-intensive non-oil-producing developing country globally [1]. Therefore, due to the stringent global environmental standards and high fuel costs, using energy-efficient and environmentally friendly systems is crucial for all South African industries. One of the significant energy consumption processes is the drying of agricultural produce such as fruits, vegetables, and nuts. The energy consumption for food preservation consumes 7–15% of total energy in developed countries and presents about 10–15% of the overall world industrial energy consumption [2–4].

However, the drying of fruits, grains, and vegetables in South Africa is still dominated by traditional drying methods such as electrical heating, diesel engine heating, and fossil fuel burning [5]. Therefore, improving the energy efficiency of drying systems should focus on the benefit of the economy, environmental protection, social sustainability, and energy supply, with a collective effort toward using energy-efficient technologies to solve the current challenges of high fuel prices, carbon dioxide emissions, and climate change facing South Africa and the rest of the world [6,7].

Heat pump drying (HPD) systems are one of the technologies used in the transition towards sustainable energy systems due to their ability to provide electricity-based drying processes at high energy efficiencies. Moreover, researchers working on food preservation recommend heat pump drying systems due to their high energy efficiency and minimal environmental impact [8–10]. It is evident that HPD systems are the future of drying systems in general, and a continuous improvement in the energy efficiency of these systems is crucial.

South Africa has sub-tropical and temperate climate conditions suitable for heat pump applications. The harvesting season, which spans from May to August, with its lower average temperature range of between 3 and 10 °C and the extreme lower temperature of about −5 °C, will, in principle, reduce the performance of a heat pump drying system to a certain degree. However, these energy-efficient and environmentally friendly systems have not been widely investigated and used in South Africa as they should have, even though the research has shown that HPD systems, which exhibit twice the efficiency of traditional hot air dryers, have the potential to substantially reduce energy consumption during drying operations [11].

An air-source heat pump (ASHP) extracts thermal energy from a low-temperature air source and transfers it to a high-temperature heat sink with less power input. The quality of the heat source is related to the temperature at which the heat can be transferred, and for an energy-efficient HPD system, the compressor should be highly efficient and well-optimised with other system components [12,13]. Therefore, enhancing the efficiency of the heat pump system involves reducing the compressor energy usage, improving the condenser heat-dissipation capability, and minimising the pressure difference between the evaporator and condenser [14].

An air-source heat pump system may be considered simple in design compared to the other heat sources for the heat pumps [15]. However, due to the fluctuations in weather conditions from season to season, the performance of an ASHP system varies significantly compared to other heat sources for the heat pump and is strongly influenced by ambient temperature [16]. Several studies conducted on the performance of ASHP systems as the climate changes suggest that it is crucial to determine the effect of ambient temperature on the performance of an ASHP. In cold environments, the efficiency of the ASHP system tends to decrease severely due to the lower volumetric efficiency of the compressor and the lower refrigerant mass flow rate [17]. For instance, Koopman et al. [18] conducted a simulation study on an air-source heat pump system using R410, R32, and R290 to evaluate the effect of pressure drop on the efficiency at an ambient temperature range from 20 °C to −10 °C. Their findings indicated that, at an ambient temperature of 20 °C, the COP increased by 35% compared to 7 °C. Conversely, at a −10 °C ambient temperature, the COP decreased by 26%.

Li et al. [19] experimentally evaluated the effect of the opening degree of the electronic expansion valve, the temperature of the low-temperature heat source at the simulated temperature ranges from −10 °C to 10 °C, and the auxiliary hot water temperature on the performance of a heat pump system. The results showed that ambient temperature was the second factor influencing the system performance. The results of the study by Bagarella et al. [20], who investigated the influence of major heat pump component sizing on the thermal performance of an HP system at varied outdoor temperatures, showed that the increased outdoor temperatures improved the heating capacity of the HP.

Ji et al. [21] studied the performance of an air-source heat pump system in cold areas, and the results showed that an air-source heat pump can withstand and operate stably at ambient temperatures as low as −25 °C. A study by Ji et al. [22] showed that the heating performance of an ASHP system with a finned-tube heat exchanger could be efficiently improved by increasing the ambient temperature and the airflow velocity. Hamid et al. [23] investigated the energy efficiency of a heat pump dryer for high-moisture-content materials. The results showed that the water-removal rate depended on the moisture diffusivity and

increased with the drying air temperature and velocity, and the higher heat transfer rate led to a higher COP.

Yu and Chan [24] conducted a study to investigate how adjusting the speed of the condenser fan impacted the performance of an air-cooled chiller. They devised an algorithm that utilised a condenser set point to calculate the appropriate fan speed to achieve an efficient heat rejection airflow. Their findings highlight that it is important to set the condensing temperature set point based on the ambient temperature and system load to optimise the system performance.

Notably, most of the available literature evaluating the effect of ambient temperature is essentially focused on HP systems for space heating and cooling, while most of the literature on heat pump drying systems mainly focuses on either the product's drying characteristics or the dryer's performance evaluation. A heat pump drying system combines two subsystems (a heat pump and a drying chamber) that work together to remove moisture from the product or material [8]. Therefore, evaluating the operability conditions and the thermal performance of heat pump drying systems for accurate sizing and energy efficiency for South African climatic conditions is crucial.

The limited literature on the operating conditions of HPD systems has left a significant gap in the guidelines for understanding the effect of several factors, such as ambient temperatures, which influence the operating conditions and the thermal performance of the HPD systems. Moreover, it is essential to understand the thermal performance and the operating conditions of an HPD system at various conditions to determine its feasibility at specific site temperatures. Hence, this experimental investigation, which assesses how ambient temperature influences operating conditions and the thermal performance of open-loop air-source HPD systems within South Africa's climate context, is valuable for research studies to analyse the performance of air-source heat pump drying systems in relation to ambient conditions.

2. Materials and Methods

2.1. Materials and Equipment

2.1.1. Heat Pump

An open-loop air-source HPD system is shown in Figure 1. This system comprises four main components, i.e., two heat exchangers (the evaporator and condenser), the semi-hermetic compressor, and the thermal expansion valve (TEV), which are integrated to make the heat pump system. The HP system was also fitted with accessories, including the liquid receiver, filter drier, solenoid valve, and sight glass. The HP system was then integrated into the batch drying chamber, which is suitable for drying agricultural biomaterials through the air circulation duct.

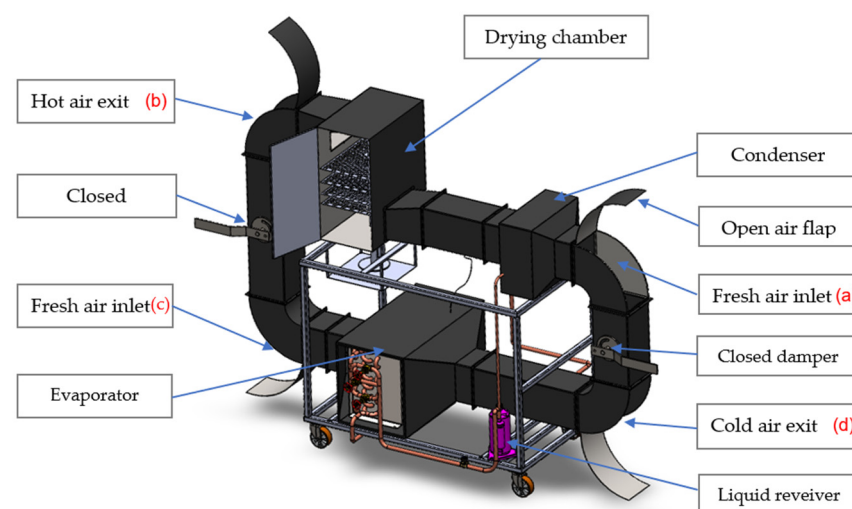


Figure 1. Three-dimensional model of an open-loop HPD system.

2.1.2. Air Duct and Drying Chamber

The diagrams in Figures 1 and 2 depict an air duct system. The air duct and the drying chamber were fabricated using a galvanised metal sheet and includes a hinged lid for product loading and unloading; moreover, insulation measures were introduced to minimise heat loss from the heat pump drying system.

2.1.3. Measurement Equipment Specifications and Data Acquisition

To evaluate the performance of the heat pump drying (HPD) system, refrigerant temperatures and pressures at various key points, the refrigerant mass flow rate, power consumption, and the climate chamber temperature were measured and collected.

A total of fifteen T-type copper thermocouples were employed to determine the refrigerant temperature and air temperatures at different positions within the HPD system and in the environmental chamber according to the recommendations by ASHRAE standard 41.1 [25], as depicted in Figure 2. The manufacturer claimed the temperature measuring range of these thermocouples to be from $-75\text{ }^{\circ}\text{C}$ to $250\text{ }^{\circ}\text{C}$ with an uncertainty of $\pm 0.1\text{ }^{\circ}\text{C}$.

As shown in Figure 2, the measurement of low and high pressures on the HP system and at the suction and delivery lines of the compressor was strategically performed following ASHRAE STANDARD 41.3 [26], which provides the frameworks on the methods for pressure measurement. The pressure transducers of model A-10 with a measuring range from 0 bar to 40 bar, and the relative uncertainty of $\pm 0.1\%$ at full scale, were used.

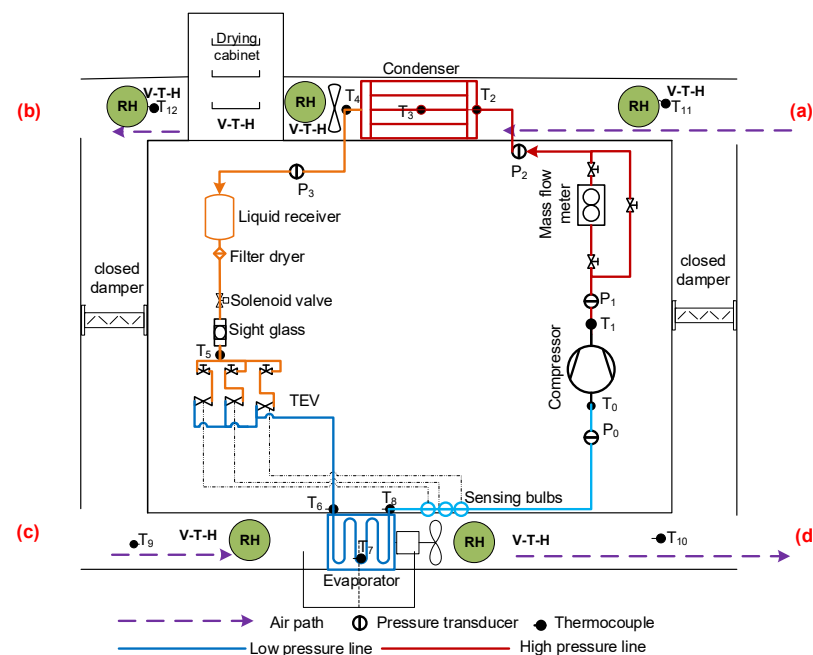


Figure 2. Schematic layout of the open-loop HPD system experimental setup, (a) fresh air inlet at the condenser side, (b) hot air discharge from the drying chamber, (c) fresh air inlet at the evaporator side, (d) cold air discharge from the evaporator.

A Coriolis mass flow meter was used to measure the refrigerant mass flow rate after the compressor and before the condenser to ensure that only the gas fluid was measured for accuracy. The mass flowmeter has a maximum operating pressure of 25 MPa, a working fluid temperature range from $-50\text{ }^{\circ}\text{C}$ to $150\text{ }^{\circ}\text{C}$, and an ambient operating temperature range from $-20\text{ }^{\circ}\text{C}$ to $70\text{ }^{\circ}\text{C}$. This mass flowmeter has a flow measuring capacity range of 0 to 100 kg/h, with a manufacturer's claimed accuracy of $\pm 0.2\%$ at the full scale and a repeatability of $\pm 0.1\%$.

2.2. Experimental Procedure

The schematic diagram of an open-loop HPD system configuration is depicted in Figure 2. This system draws in the air from the ambient environment at (c) as a heat source using the evaporator fan, passes it through the evaporator, and releases the cooler air to the ambient environment at (d). Also, the condenser fan draws the air from the ambient environment at (a) and the air is heated by the condenser. The heated air from the condenser is then fed into the drying chamber via the same fan to heat the produce, evaporate water from the produce, and move the moisture away from the produce before the air is released into the ambient environment.

The experimental setup was created to evaluate the operational conditions and the thermal performance of an open-loop air-source HPD system in different ambient temperature conditions ranging from $-10\text{ }^{\circ}\text{C}$ to $20\text{ }^{\circ}\text{C}$ at increments of $10\text{ }^{\circ}\text{C}$ in a climate chamber.

At the beginning of each experiment, all the temperature and pressure measurements were recorded and compared to ensure that all measuring instruments were accurately functional. Then, the environment chamber was set and run until the desired ambient conditions were attained. Subsequently, the HPD system was run for approximately two hours after reaching stable conditions, and then the data presented in this study were cross-sectionally sampled from those continuously recorded. The sampling was performed at increments of 30 min for 90 min after the HPD system had reached stable conditions.

The mean values of the collected temperatures and pressures were used to acquire and determine secondary data, which mainly focused on the refrigerant properties, such as the enthalpies and density, at the salient points indicated in Figure 3.

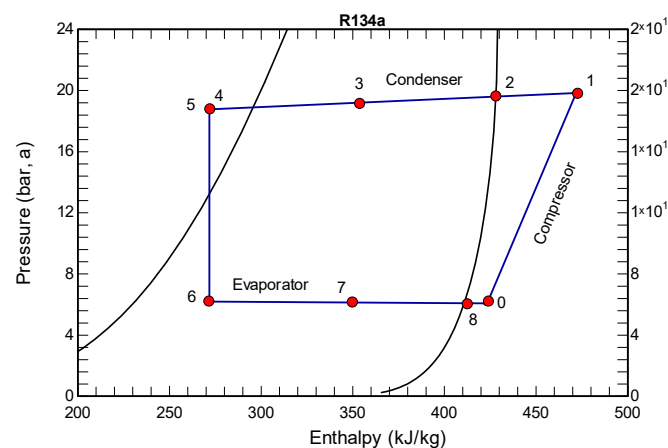


Figure 3. P-h diagram indicating the salient points used for the HP analysis.

Finally, the secondary data and primary measurements, including the refrigerant mass flow rate and power input, were used to determine tertiary data, such as the heating capacity, heating effect, compression ratio, and COP.

3. Experimentation and Uncertainty

3.1. Results and Data Analysis

The thermophysical properties of the R134a were determined at various points in the HP system, as shown in Figure 3, and the heat pump performance parameters, such as the enthalpy and density, were acquired and calculated, respectively, using the academic, professional version 10.836 (2020) of Engineering Equation Solver (EES) software.

Point 0 is the compressor suction, point 1 is the discharge from the compressor, point 2 is the entry to the condenser, point 3 is the middle point surface of the condenser coil, point 4 is the exit from the condenser, point 5 is at the inlet to the expansion valve, point 6 is the entry to the evaporator, point 7 is the middle point surface of the evaporator coil, and point 8 is just after the exit of the evaporator.

The COP for the heat pump dryer was determined by the ratio of the heating capacity to the total power consumed by the system, including the power consumption by the evaporator and condenser fans and the compressor, as given in Equation (1), and the coefficient performance of the heat pump (COP_{HP}) was computed using Equation (3).

$$COP_{HPD} = \frac{\dot{Q}_H}{(P_{comp} + P_{fan,cond} + P_{fan,evap})} \quad (1)$$

where P_{fan} is the power consumption by the fan.

The heating capacity is the product of the refrigerant mass flow rate and the enthalpy difference across the condenser, as given by Equation (3).

$$\dot{Q}_H = \dot{m}_{ref}(h_2 - h_4) \quad (2)$$

where h_2 is the specific enthalpy of the refrigerant at the inlet to the condenser (kJ/kg), h_4 is the specific enthalpy of the refrigerant at the exit of the condenser (kJ/kg), and \dot{m}_{ref} is the refrigerant mass flow rate (kg/s).

The COP_{HP} for the heat pump only was determined from Equation (4)

$$COP_{HP} = \frac{Q_{cond}}{W_{comp}} \quad (3)$$

where Q_{cond} is the heating effect or the heat rejected from the condenser (kJ/kg) and W_{comp} is specific work input by the compressor (kJ/kg).

$$Q_{cond} = (h_2 - h_4) \quad (4)$$

$$W_{comp} = (h_1 - h_0) \quad (5)$$

where h_0 is the specific enthalpy of the refrigerant at suction to the compressor (kJ/kg) and h_1 is the specific enthalpy of the refrigerant at discharge from the compressor (kJ/kg).

3.2. Uncertainties

The data analysis outlined in this article is divided into three categories, with the first category focusing on directly measured properties such as the ambient temperature, refrigerant mass flow rate, and pressures and temperatures at the inlet and outlet of all four primary components of the HP system. The maximum uncertainty in the measurement of a mass flow rate of the refrigerant is $\pm 0.2\%$ (± 0.11 kg/h), the refrigerant and ambient temperature are ± 0.1 °C ($\pm 0.75\%$), the refrigerant pressure is $\pm 0.1\%$ (± 0.02 bar), and power is $\pm 2\%$. When considering the controlled ambient temperature variation from -10 to 20 °C, the relative uncertainty of the temperature in the environmental chamber was 0.33% .

The data of the properties using the refrigerant temperature and pressure, such as the density and specific enthalpy, and the degree of superheat and subcooling, constitute the second data category. The measured pressure and temperature uncertainty were used to calculate the uncertainty of the refrigerant properties. The degree of superheat and subcooling uncertainty was 3.2% and 2.5% , respectively. The uncertainty of the specific enthalpy was computed by partial derivatives at measured temperatures and pressures. The same method was adopted to estimate the uncertainty of the refrigerant density, and the uncertainty of the specific enthalpy was 3.0% , while that of the refrigerant density was 0.8% .

The third category is the parameters calculated from the measured properties, and their errors were calculated by the uncertainty propagation formula shown in Equation (6).

$$W_R = \sqrt{\left(\frac{\partial R}{\partial x_1} w_1\right)^2 + \left(\frac{\partial R}{\partial x_2} w_2\right)^2 + \cdots + \left(\frac{\partial R}{\partial x_n} w_n\right)^2} \quad (6)$$

The result R is a function of the independent variables x_1, x_2, \dots, x_n ; W_R is the uncertainty in the result; w_1, w_2, \dots, w_n is the uncertainty in the independent variables.

The maximum uncertainties are estimated to be 0.8% and 2.9% for the heating effect and the specific work input, respectively. In contrast, the maximum uncertainty for the heating capacity, compression work, heat pump COP, and the heat pump dryer COP were 0.8%, 3.0%, 3.1%, and 3.4%, respectively.

4. Results and Discussions

4.1. Variation in the Operating Conditions of the Open HPD System with Ambient Temperatures

Figure 4 illustrates the impact of varying ambient temperatures, ranging from $-10\text{ }^{\circ}\text{C}$ to $20\text{ }^{\circ}\text{C}$, on several critical temperatures within the HP system, such as the evaporator temperature, suction temperature, discharge temperature, condenser temperature, and the temperature inside the drying chamber. A notable observation is the increase in the evaporator temperature, which increased by an average of $9.3\text{ }^{\circ}\text{C}$, moving from its lowest point of $-18.2\text{ }^{\circ}\text{C}$ to $7.6\text{ }^{\circ}\text{C}$ as the ambient temperature increased from $-10\text{ }^{\circ}\text{C}$ to $20\text{ }^{\circ}\text{C}$. Furthermore, it was observed that the evaporator temperature averaged $12.9\text{ }^{\circ}\text{C}$ lower than the ambient temperature when the ambient temperatures were above $0\text{ }^{\circ}\text{C}$. This difference between the evaporator and ambient temperatures was reduced to $4.7\text{ }^{\circ}\text{C}$ at ambient temperatures of $0\text{ }^{\circ}\text{C}$ and below. This disparity in temperature between the evaporator and ambient environment is an essential factor in facilitating heat energy extraction from the surroundings. Notably, when the ambient temperature decreased, there was a corresponding reduction in the heat energy input to the evaporator. This reduction was attributed to the diminished temperature difference between the refrigerant and the air passing through the evaporator coil from the ambient environment.

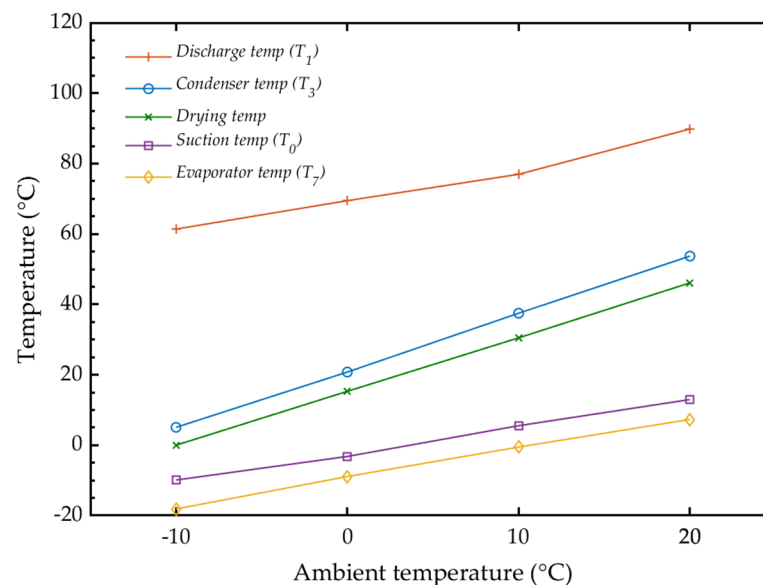


Figure 4. Effect of ambient temperature on the evaporator, suction, discharge, and condenser temperatures.

Consequently, at a lower temperature, the refrigerant absorbed less heat from the surroundings. This phenomenon is reflected in the trend of the suction temperature, which, on average, was about $5.7\text{ }^{\circ}\text{C}$ higher than the evaporator temperature.

The compressor's discharge temperature in the system consistently increased by an average of $10\text{ }^{\circ}\text{C}$, rising from an initial temperature of $60\text{ }^{\circ}\text{C}$ at an ambient temperature of $-10\text{ }^{\circ}\text{C}$ to $89.9\text{ }^{\circ}\text{C}$ when the ambient temperature was at $20\text{ }^{\circ}\text{C}$. Conversely, the increased ambient temperatures significantly increased the condenser temperatures, as evidenced by a 10.5 times improvement observed as the ambient temperatures increased from $-10\text{ }^{\circ}\text{C}$ to $20\text{ }^{\circ}\text{C}$, and from $53.7\text{ }^{\circ}\text{C}$ to $5.1\text{ }^{\circ}\text{C}$, as depicted in Figure 3. The drying temperature

followed a similar upward trajectory with increasing ambient temperatures from the lowest reading of 0 °C at an ambient temperature of −10 °C to 46.1 °C at an ambient temperature of 20 °C. Notably, on average, the drying temperatures were 5.4 °C lower than the condenser temperatures. From a drying efficiency perspective, the drying rate has a strong relationship with the drying temperature and increases with increased drying temperature [27]. Therefore, the open-loop heat pump drying system performed poorly in achieving an efficient drying temperature at ambient temperatures of 0 °C and −10 °C, as it attained drying temperatures of 15.3 °C and 0 °C, respectively.

Figure 5 shows the impact of the ambient temperature changes on the pressures in the heat pump drying system. The results indicate an increase in the suction pressure as ambient temperatures increased, with increases of 30.4%, 36.5%, and 35.7% recorded across temperature ranges from −10 °C to 0 °C, 0 °C to 10 °C, and 10 °C to 20 °C, respectively. Similarly, there was a noticeable increase in the discharge pressure by 46.8%, 51.8%, and 41.1% over the corresponding temperature intervals of −10 °C to 0 °C, 0 °C to 10 °C, and 10 °C to 20 °C, respectively. These improvements in operating pressures on the HP system were also reflected by the increased condenser pressures, as they improved by 64.5%, 60.2%, and 51.7% when the ambient temperatures increased from −10 °C to 20 °C by increments of 10 °C.

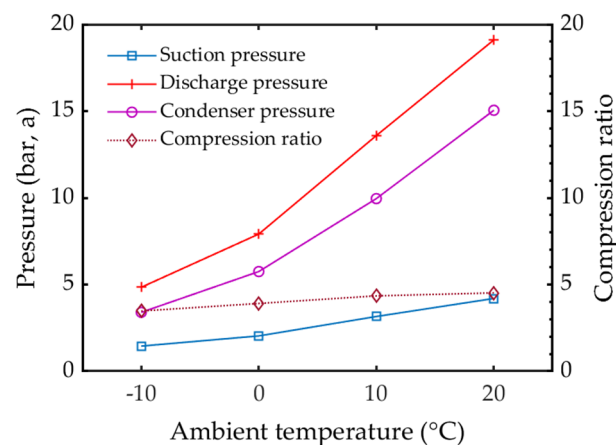


Figure 5. Variation in the pressure and pressure ratio with ambient temperature.

Hence, it can be concluded that lower ambient temperatures significantly decrease the heat pump drying system's suction pressure, discharge pressure, and condenser pressure. Notably, the rate at which the condenser pressure increased with increased ambient temperatures lowered as the ambient temperatures increased due to the decreased temperature difference between the system and the surroundings.

Most notably, at ambient temperatures above 0 °C, while the suction pressure significantly decreased, it was less sensitive to ambient temperature changes than the discharge pressure. This differential impact on the pressures led to a slight increase in the compression ratio, which increased from 3.5 at −10 °C to 4.5 at 20 °C.

Additionally, there was a decrease in the pressure drop from the compressor discharge to the condenser with lower ambient temperatures due to the decreased refrigerant mass flow. The trends observed in the suction pressure closely mirror those of the changes in the refrigerant density, as depicted in Figure 6. This correlation suggests that changes in the refrigerant properties significantly influence the operating parameters of the HP system. Furthermore, the reduced thermal energy absorbed from the environment at lower ambient temperatures results in a lower refrigerant density and, consequently, a lower suction pressure within the HP system [28].

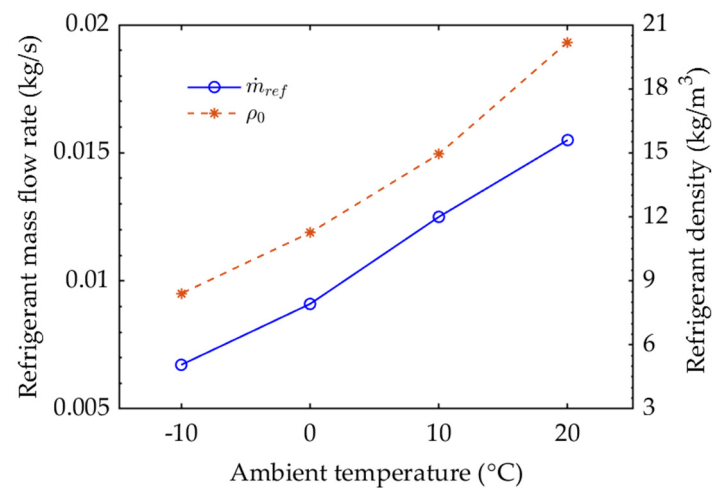


Figure 6. Variation in the mass flow and density with ambient temperature.

In this study, the displacement volume for the compressor used was fixed. As a result, the mass flow rate of the refrigerant passing through the compressor depends on the density of gases drawn into the compressor and the volumetric efficiency of the compressor. The density of a refrigerant is greatly affected by temperature and pressure variations, as they alter the kinetic movement of the refrigerant molecules and impact its mass flow rate through the compressor [28,29]. The superheated refrigerant entering the compressor of an HP system is less dense if it is at high temperatures; similarly, the increased refrigerant pressure of the superheated gasses with increased ambient temperature results in a higher density.

Figure 6 illustrates the relationship between changes in the ambient temperature and their impact on refrigerant density at the compressor's inlet point and the refrigerant mass flow rate; as the ambient temperature increased from $-10\text{ }^{\circ}\text{C}$ to $20\text{ }^{\circ}\text{C}$ in $10\text{ }^{\circ}\text{C}$ intervals, there was a corresponding increase in the refrigerant density from 20.2 kg/m^3 to 8.4 kg/m^3 , causing an increase of 24.0%, 37.4%, and 35.4% in the refrigerant mass flow rate through the compressor. The increased refrigerant density may have increased the refrigerant mass flow through the compressor, and the increased compression ratio with increased ambient temperature resulted in a decline in the volumetric efficiency of the compressor, as shown in Figure 7. Therefore, the changes in the refrigerant density directly impact the efficiency of the compressor and, consequently, the mass flow rate [28].

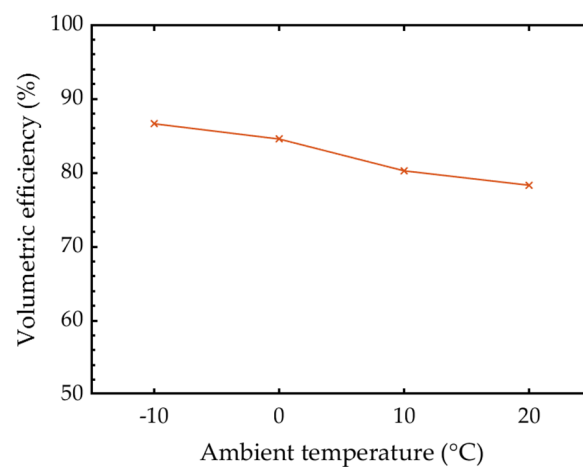


Figure 7. Variation in the volumetric efficiency with ambient temperature.

Since the suction pressure, discharge pressure, and condenser pressure decreased with the decreased ambient temperature, the HP cycle, as plotted on the p-h diagram shown in

Figure 8, lowered, consequently increasing the specific enthalpy of evaporation and the specific enthalpy of condensation.

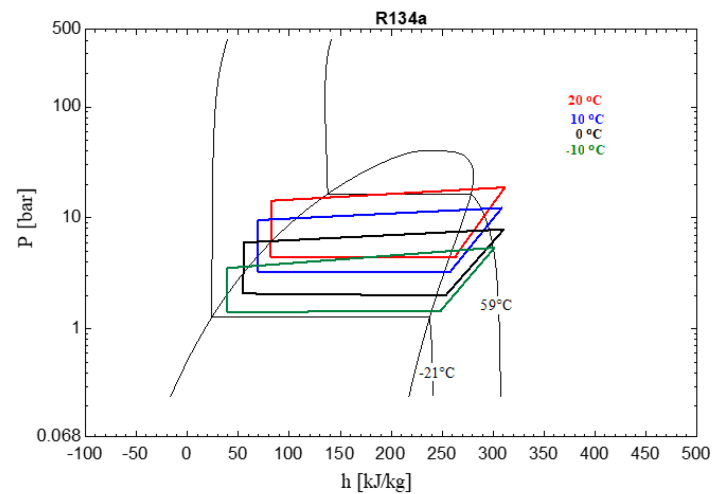


Figure 8. Effect of ambient temperature on the HP cycle.

Although the operating conditions of the HP system highly influence subcooling, the performance of a vapour compression system using subcritical refrigerants depends on the degree of subcooling [13,30]. As shown in Figure 9, the degree of subcooling increased with the decreased ambient temperature, reaching a maximum of 9.7 °C at an ambient temperature of −10 °C. Contrary to that, the degree of superheating was increased with the ambient temperature. This was due to the insignificant change in the specific enthalpy at the compressor discharge while the suction temperature increased with ambient temperature. Similar results were observed by Janković et al. [31]; hence, these results strongly suggest that decreasing the degree of superheating at the evaporator improves the COP of the system.

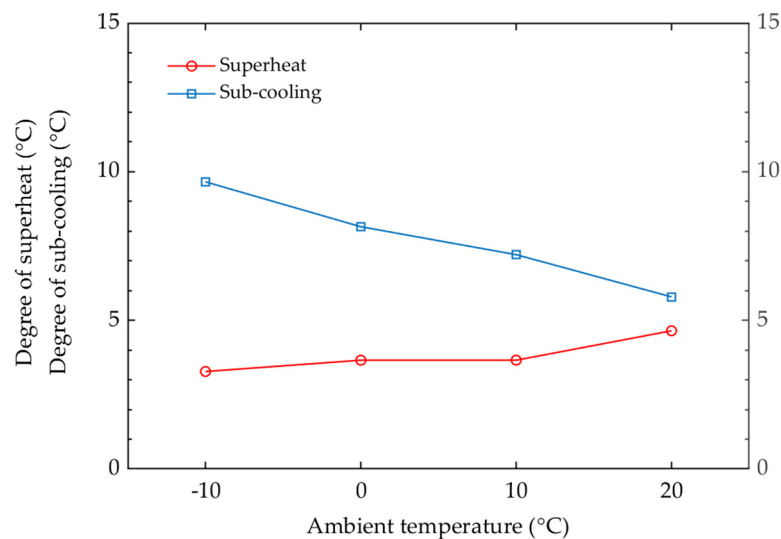


Figure 9. Influence of ambient temperature on the degree of superheat and subcooling.

4.2. Influence of Ambient Temperature on the Thermal Performance of the Heat Pump Drying System

The impact of decreased ambient temperature significantly increased the specific work performed by the compressor, as demonstrated in Figure 10. The specific work input by the compressor increased by 0.38%, 1.02%, and 1.12% as the ambient temperatures decreased from 20 to −10 °C at increments of 10 °C. This occurrence was due to the suction

temperature decreasing more rapidly than the discharge temperature. Also, the heating effect of the condenser increased with decreased ambient temperatures due to a higher specific enthalpy of condensation and increased subcooling as the heat pump (HP) cycle shifted on the pressure–enthalpy (p-h) diagram with a change in ambient temperatures.

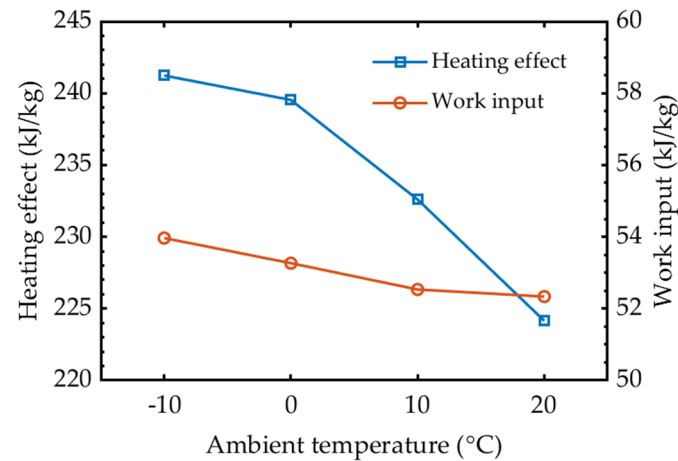


Figure 10. Influence of the ambient temperature on the heating effect and specific work input.

The findings in Figure 11 indicate how the increased ambient temperature affects the compression work, total power input, and heating capacity. A substantial overall increase of 116.7% was observed in the compression work as the ambient temperature increased from $-10\text{ }^{\circ}\text{C}$ to $20\text{ }^{\circ}\text{C}$, suggesting that, at lower temperatures, less effort was needed by the compressor to sustain the operation of the system due to the lower compression ratio and the improved volumetric efficiency of the compressor. Also, the HPD system's total power consumption increased proportionally with higher ambient temperatures. More precisely, the power consumption increased by 2.0%, 11.6%, and 12.0%, respectively, as the ambient temperature was increased in increments of $10\text{ }^{\circ}\text{C}$ from $-10\text{ }^{\circ}\text{C}$ to $20\text{ }^{\circ}\text{C}$, owing to the low density of the refrigerant at low temperatures. Consequently, the compressor needed to consume less power in order to circulate the refrigerant.

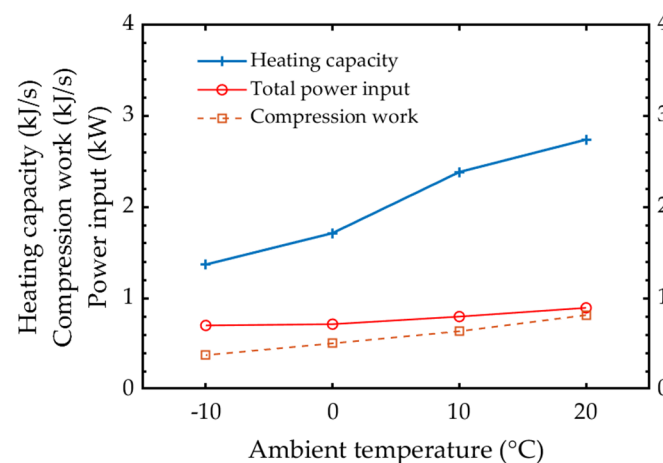


Figure 11. Variation in heating capacity, compression work, and total power input with ambient temperature.

The heating capacity of the condenser is determined by the product of the refrigerant's mass flow rate and the change in the specific enthalpy across the condenser. The heating capacity exhibited a significant increase of 26.8% from $-10\text{ }^{\circ}\text{C}$ to $0\text{ }^{\circ}\text{C}$, followed by a further increase of 25.0% from $0\text{ }^{\circ}\text{C}$ to $10\text{ }^{\circ}\text{C}$, and finally increased by 14.3% as the temperature increased from $10\text{ }^{\circ}\text{C}$ to $20\text{ }^{\circ}\text{C}$. The increases in heating capacity closely mirrored the

refrigerant mass flow rate trend, affirming a similar result trend that was also observed by Prabakaran et al. [32].

The COP is an essential criterion for measuring the thermal performance of a heat pump drying system. The COP of the HPD system is defined as the ratio of the heating capacity of the condenser to the total power consumed by the HP system. A high heating efficiency of the HPD system is indicated by a high value of the COP [33]. The COP of the heat pump drying system was lowest at $-10\text{ }^{\circ}\text{C}$ with a minimum value of 2.3, which then increased by 24.4%, 12.0%, and 2.0% as the ambient temperature increased in intervals of $10\text{ }^{\circ}\text{C}$ from $-10\text{ }^{\circ}\text{C}$ to $20\text{ }^{\circ}\text{C}$, as depicted in Figure 12. These results suggest that the open-loop HPD system has poor thermal performance at ambient temperatures of $0\text{ }^{\circ}\text{C}$ and below, and it increases with increased ambient temperatures.

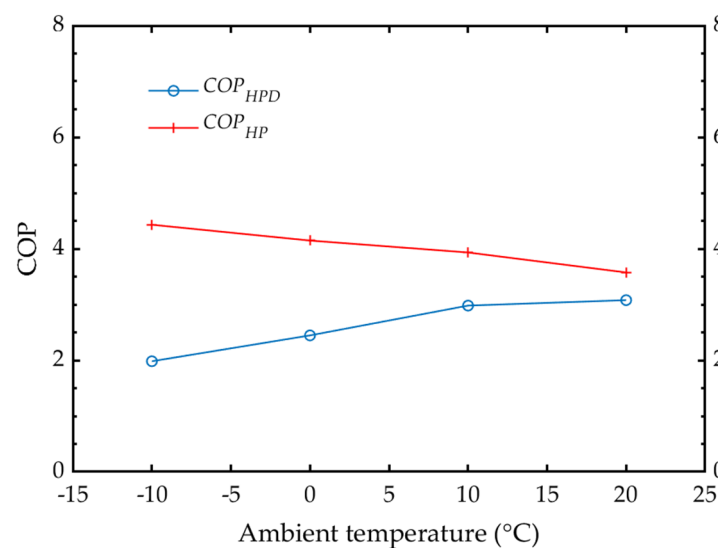


Figure 12. Variation in the COP with ambient temperature.

Moreover, as noticed in Figure 10, the heating effect decreased with the increase in the ambient temperature, and so did the specific work input by the compressor. Consequently, the heat pump COP gradually decreased by an average of 6.3% from an ambient temperature of $-10\text{ }^{\circ}\text{C}$ to $20\text{ }^{\circ}\text{C}$, as shown in Figure 12.

5. Conclusions

This experimental study investigated the influence of ambient temperatures, ranging from $-10\text{ }^{\circ}\text{C}$ to $20\text{ }^{\circ}\text{C}$ with $10\text{ }^{\circ}\text{C}$ intervals, on the operating conditions and thermal efficiency of an open-loop air-source HPD system utilising R134a refrigerant. The analysis of the findings from this study may be summarised as follows:

- (i) Lower ambient temperatures result in diminished evaporator, suction, and discharge temperatures.
- (ii) These results have shown that, although the refrigerant density may generally decrease with temperature, the second property to determine the state of the refrigerant, such as the pressure, was also a significant property.
- (iii) The higher rate of increase in the discharge pressure with ambient temperatures compared to the suction pressure, which increased the compression ratio, negatively influenced the volumetric efficiency of the compressor.
- (iv) The power consumption by the compressor is highly dependent on the refrigerant mass flow rate, and the heating capacity greatly influences the COP_{HPD} .
- (v) At ambient temperatures below $10\text{ }^{\circ}\text{C}$, the COP of the open HPD system decreased significantly, indicating the reduced energy efficiency of an open-loop air-source HPD system in such conditions.

Therefore, these results conclude that employing an open-loop HPD system is feasible in South African climatic conditions. However, its practical use is limited to warmer regions, or it may be used during warm seasons, because the system's effectiveness highly depends on ambient temperature factors, affecting its operating conditions, thermal efficiency, and moisture-extraction capability. Therefore, further study could explore alternative HPD system configurations or refrigerants to expand the suitability across various climatic conditions nationwide.

Author Contributions: S.M.N.: Conceptualisation; methodology; software; validation; formal analysis; investigation; resources; data curation; visualisation; writing—original draft preparation. Z.H.: writing—review and editing; supervision; project administration; funding acquisition. All authors have read and agreed to the published version of the manuscript.

Funding: This research was partly funded by the National Research Foundation of South Africa (Ref Number: BAAP2204254744).

Data Availability Statement: The original contributions presented in the study are included in the article, further inquiries can be directed to the corresponding author.

Conflicts of Interest: The authors declare no conflicts of interest.

Abbreviations

The following abbreviations are used in this manuscript:

ASHRAE	American Society of Heating, Refrigerating, and Air-Conditioning Engineers
COP	Coefficient of performance
EES	Engineering Equation Solver
HP	Heat pump
HPD	Heat pump dryer
TEV	Thermal expansion valve
\dot{m}_{ref}	Refrigerant mass flow rate (kg/s)
h	Specific enthalpy (kJ/kg)
P	Power ((kJ/s) or (kW))
p	Absolute pressure (bar, a)
\dot{Q}	Heating capacity (kJ/s)
Q	Heating effect (kJ/kg)
t	Temperature (°C)
W	Work (kJ/kg)
Subscripts	
Comp	Compressor
Cond	Condenser
Evap	Evaporator
ref	Refrigerant
ρ	Density
\emptyset	Diameter
η	Efficiency

References

1. Ishaku, H.P.; Adun, H.; Jazayeri, M.; Kusaf, M. Decarbonisation Strategy for Renewable Energy Integration for Electrification of West African Nations: A Bottom-Up EnergyPLAN Modelling of West African Power Pool Targets. *Sustainability* **2022**, *14*, 15933. [\[CrossRef\]](#)
2. Yousaf, K.; Chen, K.; Khan, M.A. An Introduction of Biomimetic System and Heat Pump Technology in Food Drying Industry. In *Biomimetics*; IntechOpen: London, UK, 2020.
3. Sansaniwal, S.K.; Sharma, V.; Mathur, J. Energy and exergy analyses of various typical solar energy applications: A comprehensive review. *Renew. Sustain. Energy Rev.* **2018**, *82*, 1576–1601. [\[CrossRef\]](#)
4. El Hage, H.; Herez, A.; Ramadan, M.; Bazzi, H.; Khaled, M. An investigation on solar drying: A review with economic and environmental assessment. *Energy* **2018**, *157*, 815–829. [\[CrossRef\]](#)
5. Kivevele, T.; Huan, Z. A review on opportunities for the development of heat pump drying systems in South Africa. *S. Afr. J. Sci.* **2014**, *110*, 37–47. [\[CrossRef\]](#)

6. Wang, L. Energy efficiency technologies for sustainable food processing. *Energy Effic.* **2014**, *7*, 791–810. [\[CrossRef\]](#)
7. Shah, N.; Huang, M.; Hewitt, N.J. Performance analysis of diesel engine heat pump incorporated with heat recovery. *Appl. Therm. Eng.* **2016**, *108*, 181–191. [\[CrossRef\]](#)
8. Chua, K.J.; Chou, S.K.; Yang, W.M. Advances in heat pump systems: A review. *Appl. Energy* **2010**, *87*, 3611–3624. [\[CrossRef\]](#)
9. Tunckal, C.; Doymaz, İ. Performance analysis and mathematical modelling of banana slices in a heat pump drying system. *Renew. Energy* **2020**, *150*, 918–923. [\[CrossRef\]](#)
10. Fan, H.; Shao, S.; Tian, C. Performance investigation on a multi-unit heat pump for simultaneous temperature and humidity control. *Appl. Energy* **2014**, *113*, 883–890. [\[CrossRef\]](#)
11. Fayose, F.; Huan, Z. Heat Pump Drying of Fruits and Vegetables: Principles and Potentials for Sub-Saharan Africa. *Int. J. Food Sci.* **2016**, *2016*, 9673029. [\[CrossRef\]](#)
12. Choi, J.M.; Kim, Y.C. The effects of improper refrigerant charge on the performance of a heat pump with an electronic expansion valve and capillary tube. *Energy* **2002**, *27*, 391–404. [\[CrossRef\]](#)
13. Pitarch, M.; Hervás-Blasco, E.; Navarro-Peris, E.; Corberán, J.M. Exergy analysis on a heat pump working between a heat sink and a heat source of finite heat capacity rate. *Int. J. Refrig.* **2019**, *99*, 337–350. [\[CrossRef\]](#)
14. Elsayed, A.O.; Hariri, A.S. Effect of condenser air flow on the performance of split air conditioner. In Proceedings of the World Renewable Energy Congress-Sweden, Linköping, Sweden, 8–13 May 2011; Linköping University Electronic Press: Linköping, Sweden, 2011; pp. 2134–2141.
15. Sezen, K.; Gungor, A. Performance analysis of air source heat pump according to outside temperature and relative humidity with mathematical modeling. *Energy Convers. Manag.* **2022**, *263*, 115702. [\[CrossRef\]](#)
16. Carroll, P.; Chesser, M.; Lyons, P. Air Source Heat Pumps field studies: A systematic literature review. *Renew. Sustain. Energy Rev.* **2020**, *134*, 110275. [\[CrossRef\]](#)
17. Wu, C.; Liu, F.; Li, X.; Wang, Z.; Xu, Z.; Zhao, W.; Yang, Y.; Wu, P.; Xu, C.; Wang, Y. Low-temperature air source heat pump system for heating in severely cold area: Long-term applicability evaluation. *Build. Environ.* **2022**, *208*, 108594. [\[CrossRef\]](#)
18. Koopman, T.; Zhu, T.; Rohlf, W. Performance evaluation of air-source heat pump based on a pressure drop embedded model. *Heliyon* **2024**, *10*, e24634. [\[CrossRef\]](#) [\[PubMed\]](#)
19. Li, X.; Wang, Y.; Li, M.; Hang, M.; Zhao, W.; Kong, D.; Yin, G. Performance testing of a heat pump system with auxiliary hot water under different ambient temperatures. *Energy Built Environ.* **2022**, *3*, 316–326. [\[CrossRef\]](#)
20. Bagarella, G.; Lazzarin, R.; Noro, M. Sizing strategy of on-off and modulating heat pump systems based on annual energy analysis. *Int. J. Refrig.* **2016**, *65*, 183–193. [\[CrossRef\]](#)
21. Ji, S.; Liu, Y.; Xu, H.; Yang, Y.; Chen, J.; Xue, K.; Sun, Y. Application and Analysis of Air-Source Heat Pump Heat Supply System in Cold Areas. *J. Phys. Conf. Ser.* **2022**, *2186*, 012017. [\[CrossRef\]](#)
22. Ji, W.; Cai, J.; Ji, J.; Huang, W. Experimental study of a direct expansion solar-assisted heat pump (DX-SAHP) with finned-tube evaporator and comparison with conventional DX-SAHP. *Energy Build.* **2020**, *207*, 109632. [\[CrossRef\]](#)
23. Hamid, K.; Sajjad, U.; Yang, K.S.; Wu, S.-K.; Wang, C.-C. Assessment of an energy efficient closed loop heat pump dryer for high moisture contents materials: An experimental investigation and AI based modelling. *Energy* **2022**, *238*, 121819. [\[CrossRef\]](#)
24. Yu, F.W.; Chan, K.T. Advanced control of heat rejection airflow for improving the coefficient of performance of air-cooled chillers. *Appl. Therm. Eng.* **2006**, *26*, 97–110. [\[CrossRef\]](#)
25. ANSI/ASHRAE Standard 41.1-2013; Standard Method for Temperature Measurement. ASHRA: Atlanta, GA, USA, 2013.
26. ANSI/ASHRAE Standard 41.3-2014; Standard Method for Pressure Measurement. ASHRA: Atlanta, GA, USA, 2014.
27. Ndukwu, M.C. Effect of drying temperature and drying air velocity on the drying rate and drying constant of cocoa bean. *Agric. Eng. Int. CIGR J.* **2009**, *6*.
28. Ngalonkulu, S.M.; Huan, Z. The influence of ambient temperature and fan speed on the operating conditions of an open-loop heat pump drying system. In Proceedings of the International Heat Transfer Conference Digital Library, Cape Town, South Africa, 14–18 August 2023; Begel House Inc.: Danbury, CT, USA. [\[CrossRef\]](#)
29. Prapainop, R.; Suen, K.O. Effects of refrigerant properties on refrigerant performance comparison: A review. *Int. J. Eng. Res. Appl.* **2012**, *2*, 486–493.
30. Hervás-Blasco, E.; Pitarch, M.; Navarro-Peris, E.; Corberán, J.M. Study of different subcooling control strategies in order to enhance the performance of a heat pump. *Int. J. Refrig.* **2018**, *88*, 324–336. [\[CrossRef\]](#)
31. Janković, Z.; Sieres, J.; Cerdeira, F.; Pavković, B. Analysis of the impact of different operating conditions on the performance of a reversible heat pump with domestic hot water production. *Int. J. Refrig.* **2018**, *86*, 282–291. [\[CrossRef\]](#)
32. Prabakaran, R.; Lal, D.M.; Kim, S.C. A state of art review on future low global warming potential refrigerants and performance augmentation methods for vapour compression based mobile air conditioning system. *J. Therm. Anal. Calorim.* **2023**, *148*, 417–449. [\[CrossRef\]](#)
33. Alishah, A.; Kiamahalleh, M.V.; Yousefi, F.; Emami, A.; Kiamahalleh, M.V. Solar-assisted heat pump drying of coriander: An experimental investigation. *Int. J. Air-Cond. Refrig.* **2018**, *26*, 1850037. [\[CrossRef\]](#)

Disclaimer/Publisher’s Note: The statements, opinions and data contained in all publications are solely those of the individual author(s) and contributor(s) and not of MDPI and/or the editor(s). MDPI and/or the editor(s) disclaim responsibility for any injury to people or property resulting from any ideas, methods, instructions or products referred to in the content.